

# Characterization of Monodisperse Copolymer Submicrospheres with Branched Structures and Different Glass-Transition Temperatures Prepared by Soap-Free Emulsion Polymerization

Yi-Yu Liu, Ming-Yu Lo, Hui Chen

Department of Chemical and Materials Engineering, National Central University, 300 Jhongda Road, Jhongli 32001, Taiwan

Received 21 December 2009; accepted 26 August 2010

DOI 10.1002/app.33362

Published online 12 January 2011 in Wiley Online Library (wileyonlinelibrary.com).

**ABSTRACT:** This study was focused on the synthesis of monodisperse poly(*n*-butyl methacrylate-*co*-methyl methacrylate) submicrospheres via soap-free emulsion polymerization and on their characterization. The glass-transition temperatures of poly(*n*-butyl methacrylate) and poly(methyl methacrylate) were approximately 25 and 110°C, respectively. Therefore, submicrospheres with different glass-transition temperatures could be obtained through the variation of the copolymer composition. In addition, relationships between the monomer feed concentration ( $M_0$ ) and the Mark-Houwink constant ( $\alpha$ ) for the copolymer submicrospheres were proposed. The molecular weights of the copolymer submicrospheres decreased sharply with an increase in the weight fraction of *n*-butyl

methacrylate. On the contrary, the particle diameter increased linearly from 277 to 335 nm with an increase in the weight fraction of *n*-butyl methacrylate. The  $\alpha$  values decreased with an increase in  $M_0$ , and this indicated that the branched structures of the copolymer submicrospheres were easily obtained when  $M_0$  was higher than 0.11 g/mL of water. Consequently, the results of this study are expected to provide useful information for the synthesis of monodisperse copolymer submicrospheres by soap-free emulsion polymerization. © 2011 Wiley Periodicals, Inc. *J Appl Polym Sci* 120: 2945–2953, 2011

**Key words:** branched; colloids; emulsion polymerization; glass transition

## INTRODUCTION

Monodisperse polymer particles have attracted considerable attention because they have potential applications in various fields such as colloid science, optics, and biotechnology.<sup>1–7</sup> Monodisperse polymer particles have also been used to prepare advanced materials such as photonic crystals.<sup>8–14</sup> The unique photonic bandgap in photonic crystals prevents the propagation of electromagnetic waves in a particular frequency range through the crystal structure.<sup>9,12</sup> Monodisperse polymer particles have been synthesized by different polymerization processes, including emulsion polymerization,<sup>15</sup> dispersion polymerization,<sup>16,17</sup> suspension polymerization,<sup>18</sup> and soap-free emulsion polymerization.<sup>19–22</sup> Among these, soap-free emulsion polymerization is the simplest method for synthesizing self-assembled monodisperse polymer particles that can be used in photonic crystals.

Ou et al.<sup>23</sup> synthesized monodisperse polymer spheres with different particle diameters and proposed different mechanisms for the nucleation process occurring during the polymerization reaction. They obtained microspheres (270–750 nm) via soap-free emulsion polymerization with styrene, potassium persulfate (KPS), and water (H<sub>2</sub>O) in a polar or nonpolar solvent or in the presence of a hydrophilic comonomer. Gu et al.<sup>19</sup> and Nagao et al.<sup>20</sup> synthesized monodisperse particles of different sizes by soap-free emulsion polymerization in a pH-controlled system. On the other hand, for the synthesis of monodisperse copolymer submicrospheres to be used in photonic crystals, Zhang et al.<sup>24</sup> and Gu et al.<sup>25</sup> proposed a rapid soap-free emulsion polymerization process in which monomers are polymerized at the boiling point of the solvent. In this method, the sizes of the monodisperse copolymer submicrospheres can be well controlled. Furthermore, a few studies have reported the synthesis of monodisperse copolymer submicrospheres with various glass-transition temperature ( $T_g$ ) values.

The quantitative analysis of monodisperse copolymer submicrospheres with different particle diameters and  $T_g$  values in the synthesis of composite

Correspondence to: H. Chen (huichen@cc.ncu.edu.tw).

Contract grant sponsor: National Science Council of Taiwan.

polymer matrices would be an interesting topic of research. For example, methyl methacrylate (MMA) and *n*-butyl methacrylate (nBMA) can be copolymerized to obtain polymers with various  $T_g$  values. Theoretically, it has been stated that  $T_g$  of a random copolymer prepared from nBMA and MMA can be varied according to the Fox equation:<sup>26</sup>

$$\frac{1}{T_g} = \frac{W_{\text{nBMA}}}{T_{g,\text{PnBMA}}} + \frac{W_{\text{MMA}}}{T_{g,\text{PMMA}}} \quad (1)$$

where  $W$  is the weight fraction of a given monomer and  $T_g$  is the glass-transition temperature of a given homopolymer or copolymer [the  $T_g$  values of poly(*n*-butyl methacrylate) (PnBMA) and poly(methyl methacrylate) (PMMA) are 26.3 and 116°C, respectively].

This article presents the synthesis of monodisperse copolymer submicrospheres by soap-free emulsion polymerization and their characterization. The compositions, weight-average molecular weight ( $M_w$ ) values,  $T_g$  values, morphologies, particle diameters, and particle size distributions of the copolymer submicrospheres prepared under various reaction conditions [the weight fraction of nBMA with respect to MMA and the monomer feed concentration ( $M_0$ )] were determined. Furthermore, the distinct relationships between the characteristics of the copolymer particles and the synthesis conditions were investigated and used to obtain polymer spheres with different physical properties that could be employed in various fields. Therefore, the results of this study are expected to provide useful information for the synthesis of monodisperse copolymer submicrospheres by soap-free emulsion polymerization.

## EXPERIMENTAL

### Materials

The MMA monomer (Showa, Okinawa, Japan) and nBMA monomer (Showa) were purified by vacuum distillation and stored at 4°C until use. KPS (Showa) was used as an initiator for polymerization without purification. H<sub>2</sub>O was subjected to reverse osmosis and deionized (DI) for an electric resistance higher than 18 MΩ cm.

### Polymerization method

Copolymer submicrospheres with various  $T_g$  values were prepared via soap-free emulsion polymerization. A typical polymerization procedure was as follows: 90 mL of DI H<sub>2</sub>O was added to a three-necked flask equipped with a reflux condenser and a mechanical stirrer. After deoxygenation with nitrogen for 30 min, KPS (0.0873 g) was added to the

**TABLE I**  
Synthesis Conditions for Soap-Free Emulsion Polymerization

Sample code	Weight fraction of nBMA	$M_0$ (g/mL of H <sub>2</sub> O)	nBMA (g)	MMA (g)
P0	0	0.11	0	10
P0.1	0.10	0.11	1	9
P0.25	0.25	0.11	2.5	7.5
P0.5	0.50	0.11	5	5
P0.75	0.75	0.11	7.5	2.5
P1	1	0.11	10	0
P0-11	0	0.11	0	10
P0-17	0	0.17	0	15
P0-22	0	0.22	0	20
P0-28	0	0.28	0	25
P0-33	0	0.33	0	30
P0-44	0	0.44	0	40
P0.5-11	0.5	0.11	5	5
P0.5-17	0.5	0.17	7.5	7.5
P0.5-22	0.5	0.22	10	10
P0.5-28	0.5	0.28	12.5	12.5
P0.5-33	0.5	0.33	15	15
P0.5-44	0.5	0.44	20	20

The conditions were as follows: 90 mL of DI H<sub>2</sub>O, 0.0873 g of KPS, a reaction temperature of 70°C, and a reaction time of 24 h.

flask under stirring. Subsequently, the six various weight fractions of nBMA with respect to MMA (10 g in total) and the six  $M_0$  values (P0 and P0.5 series) were used as shown in Table I. The temperature of the synthetic solution was increased to 70°C for 24 h under a continuous nitrogen purge at an impeller speed of 400 rpm. After the polymerization process was completed, the copolymer submicrospheres were purified with DI H<sub>2</sub>O to remove impurities by a centrifugal technique.

### Measurements

Proton nuclear magnetic resonance (<sup>1</sup>H-NMR) spectra (500-MHz Avance, Bruker, Karlsruhe, Germany) were recorded with CDCl<sub>3</sub> as the solvent in 5-mm NMR tubes. The residual <sup>1</sup>H signal in CDCl<sub>3</sub> was used as the reference in all the spectra.

The  $M_w$  values were determined via gel permeation chromatography/differential viscometry (GPC-VIS; TDA 300 and T50A, Viscotek, Houston, Texas). The instrument consisted of a pump, three 300-mm mixed columns (model KF-805L, Shodex, Tokyo, Japan), a differential refractive-index detector, and a differential pressure viscometer mounted in series. Data were collected and analyzed with Viscotek's TriSEC gel permeation chromatography software package. The GPC-VIS system was operated at 40°C with tetrahydrofuran as an eluent at 1 mL/min. The samples were prepared at a concentration of 15 mg/mL. A molecular weight calibration curve was obtained with polystyrene standards.

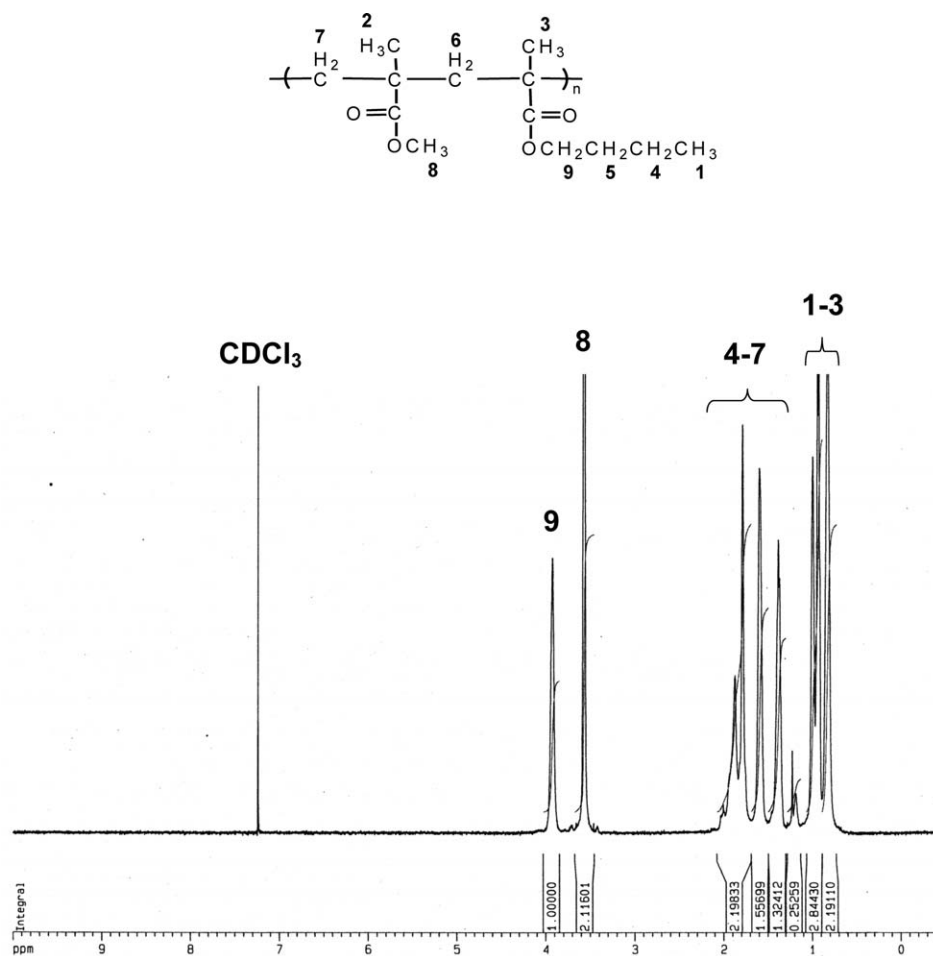


Figure 1  $^1\text{H}$ -NMR spectrum (500 MHz) of copolymer submicrospheres in the P0.5 series.

The  $T_g$  values were determined with a DSC 7 differential scanning calorimeter (PerkinElmer, Waltham, Massachusetts). The samples were kept at  $200^\circ\text{C}$  for 10 min, and then they were cooled quickly to  $-15^\circ\text{C}$  from the melt of the first scan. The  $T_g$  values were obtained as the inflection points of the heat capacity jump at a scan rate of  $10^\circ\text{C}/\text{min}$  from  $-15$  to  $160^\circ\text{C}$  during the second scan. All measurements were conducted in a nitrogen atmosphere.

More than 100 particle diameters were measured for each reacted solution with field emission scanning electron microscopy (FESEM; model S80, Hitachi, Tokyo, Japan) to determine the morphology, number-average diameter ( $\bar{d}_n$ ), volume-average diameter ( $\bar{d}_v$ ), standard deviation ( $\sigma$ ), and coefficient of variation of the particle size distribution ( $C_v$ ).<sup>19,20</sup>

$$\bar{d}_n = \left( \frac{\sum n_i d_i}{\sum n_i} \right) \quad (2)$$

$$\bar{d}_v = \left( \frac{\sum n_i d_i^3}{\sum n_i} \right)^{1/3} \quad (3)$$

$$\sigma = \left( \frac{\sum (d_i - \bar{d}_n)^2}{\sum n_i} \right)^{1/2} \quad (4)$$

$$C_v = \frac{\sigma}{\bar{d}_n} \times 100 \quad (5)$$

where  $n_i$  is the number of particles with diameter  $d_i$ . Furthermore, the number of polymer particles ( $N_P$ ) was calculated as follows:<sup>27</sup>

$$N_P = 6W_{is}/\rho\pi\bar{d}_v^3 \quad (6)$$

where  $W_{is}$  is the weight of polymer particles per reaction volume and  $\rho$  is the density of the polymer (PMMA =  $1.19 \text{ g}/\text{cm}^3$ , PnBMA =  $1.05 \text{ g}/\text{cm}^3$ ), which was determined from various compositions to be between  $1.05$  and  $1.19 \text{ g}/\text{cm}^3$ .

## RESULTS AND DISCUSSION

### Characterization of the submicrospheres

Copolymer submicrospheres were synthesized with different weight fractions of nBMA. The compositions,  $M_w$  values,  $T_g$  values, morphologies, particle diameters, and particle size distributions of the obtained copolymer submicrospheres were determined. The

TABLE II  
Properties of the Copolymer Submicrospheres

	P0	P0.1	P0.25	P0.5	P0.75	P1
$M_w \times 10^4$ (g/mol)	66.5	60.5	53.2	50.2	44.0	42.6
$T_g$ (°C)	116	103	91.9	58.4	43.6	26.3
$d_v$ (nm)	277	283	298	317	335	356 <sup>a</sup>
$C_v$ (%)	2.92	2.71	2.69	2.58	2.43	—
$N_p \times 10^{15}$ (m <sup>-3</sup> )	7.76	7.49	6.33	5.14	4.29	2.91 <sup>a</sup>

<sup>a</sup> Theoretical data from Figure 5 obtained with a linear equation.

compositions of the copolymers were determined with <sup>1</sup>H-NMR measurements. A typical <sup>1</sup>H-NMR spectrum of the copolymer submicrospheres (P0.5) is shown in Figure 1. The spectrum shows the charac-

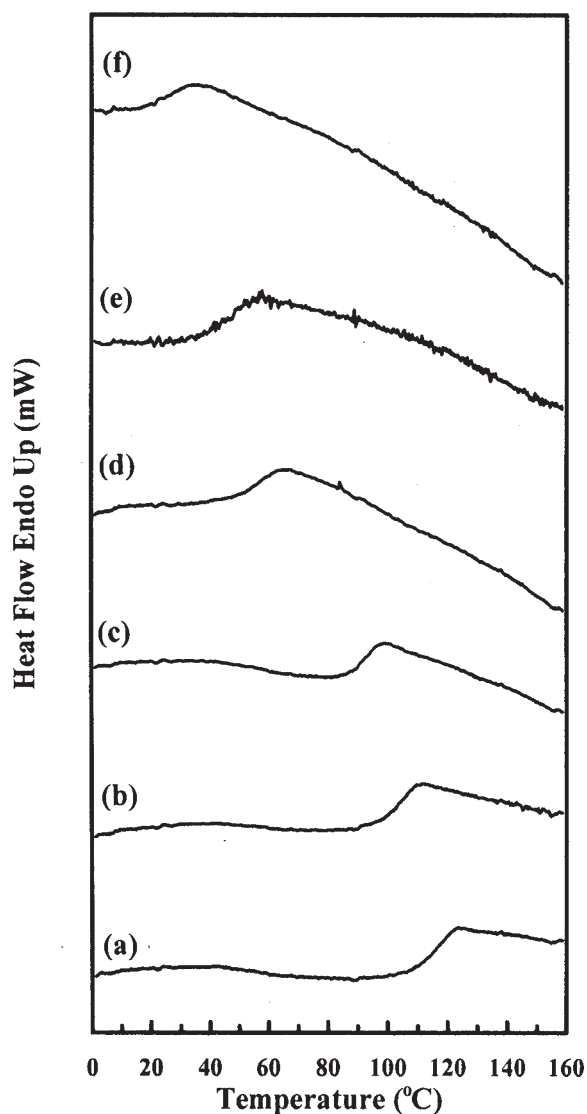


Figure 2 DSC curves of copolymer submicrospheres with various weight fractions of nBMA: (a) 0, (b) 0.1, (c) 0.25, (d) 0.5, (e) 0.75, and (f) 1.

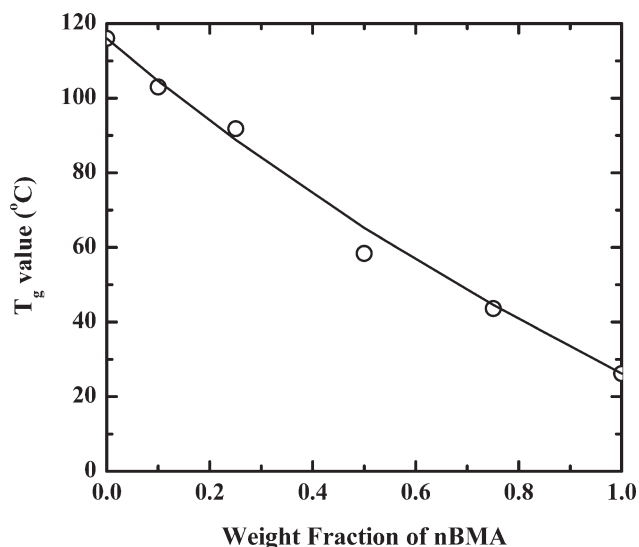
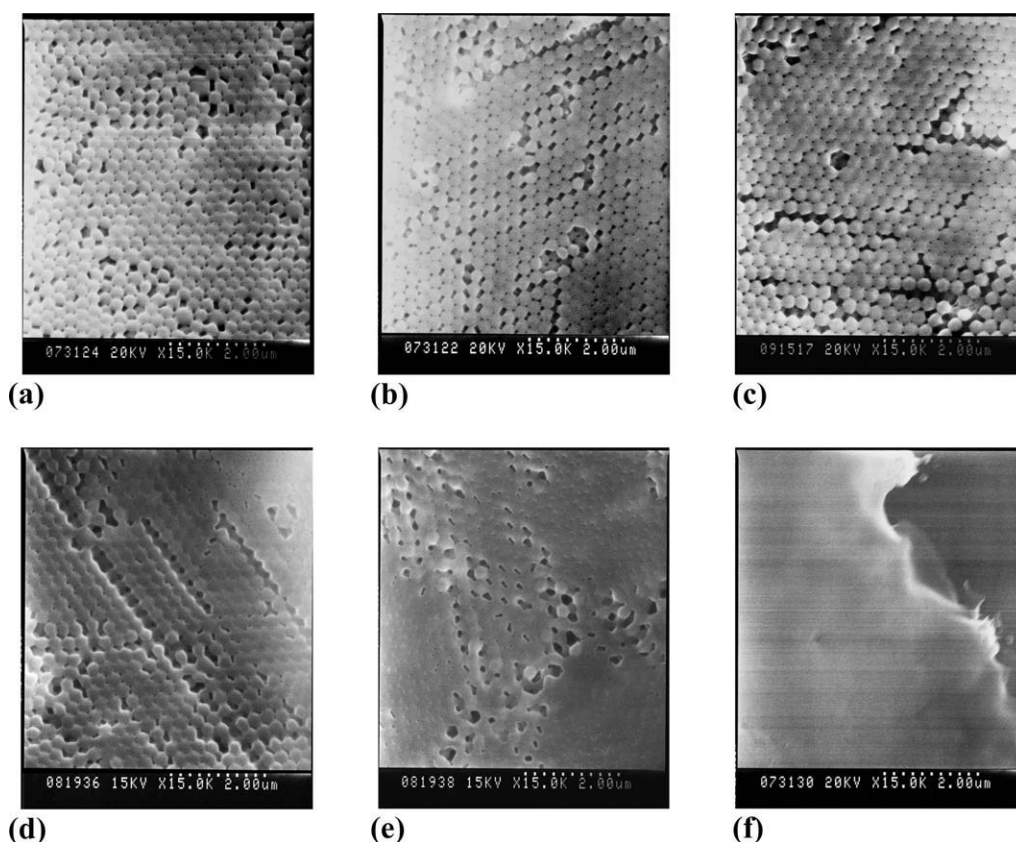


Figure 3  $T_g$  as a function of the weight fraction of nBMA. Experimental data are compared with (—) those predicted with the Fox equation ( $R^2 = 0.990$ ).

teristic peaks and integration areas corresponding to poly(*n*-butyl methacrylate-*co*-methyl methacrylate). The signals centered at 3.93 (integration area = 1.00) and 3.57 ppm (integration area = 2.12) correspond to the methylene and methyl protons adjacent to the ester oxygen of nBMA and MMA units, respectively.<sup>28</sup> Furthermore, the final copolymer composition was calculated with the aid of integration areas, and the weight fraction of nBMA units in the copolymer was determined to be 0.5. These results indicate that the initial monomer ratio was consistent with the composition of the final copolymer.

Table II shows the  $M_w$  values of copolymer submicrospheres with various weight fractions of nBMA. The PMMA (P0) and PnBMA (P1) values were  $66.5 \times 10^4$  and  $42.6 \times 10^4$  g/mol, respectively. The  $M_w$  values of the copolymer submicrospheres decreased sharply with an increase in the weight fraction of nBMA.

In soap-free emulsion polymerization, the weight fraction of nBMA is an important parameter that helps control  $T_g$  of the copolymer submicrospheres and thus determines their applicability in different fields. In this study, copolymer submicrospheres with various weight fractions of nBMA were measured by differential scanning calorimetry (DSC), as shown in Figure 2 and Table II. Apparently, with an increase in the weight fraction of nBMA from 0 to 1, the  $T_g$  values of the copolymer submicrospheres decreased from 116 to 26.3°C. Thus, monodisperse copolymer submicrospheres with various  $T_g$  values were successfully prepared by soap-free emulsion polymerization. Figure 3 shows the plots of the experimental  $T_g$  values (determined by DSC) and theoretical  $T_g$  values (calculated with the Fox equation) against the weight fractions of nBMA. The



**Figure 4** FESEM images of copolymer submicrospheres with various weight fractions of nBMA: (a) 0, (b) 0.1, (c) 0.25, (d) 0.5, (e) 0.75, and (f) 1.

theoretical values could be used to predict the experimental values, and the physicochemical properties of the obtained copolymers could be controlled by adjustments of the weight fraction of nBMA.<sup>29,30</sup>

The FESEM micrographs in Figure 4 show the morphologies of copolymer submicrospheres with various weight fractions of nBMA. The particles were uniform and spherical; moreover, the particle diameters of the copolymer submicrospheres were of the order of several hundred nanometers, and they increased with the weight fraction of nBMA. However, the shapes of the copolymer submicrospheres when the weight fraction of nBMA was 100% (P1) could not be confirmed from their FESEM image. The P1 submicrospheres were easily flattened at room temperature because of their low  $T_g$  (26.3°C). For an accurate estimation of the particle diameter, the average diameter of more than 100 particles was estimated from the FESEM micrographs. The calculated  $\bar{d}_v$ ,  $C_v$ , and  $N_p$  values are shown in Table II. The  $C_v$  values of copolymer submicrospheres with various weight fractions of nBMA were less than 3.0%, and this indicated the successful formation of monodisperse copolymer submicrospheres by soap-free emulsion polymerization. The  $\bar{d}_v$  values of the copolymer submicrospheres increased with the weight fraction of nBMA. The  $N_p$  values of the copolymer

submicrospheres were calculated with eq. (6); the results indicated that  $N_p$  decreased with an increase in the weight fraction of nBMA.

Figure 5 shows the relationship between  $\bar{d}_v$  and  $N_p$  for copolymer submicrospheres with various weight fractions of nBMA. When the weight fraction of nBMA was increased from 0 to 0.75,  $\bar{d}_v$  increased

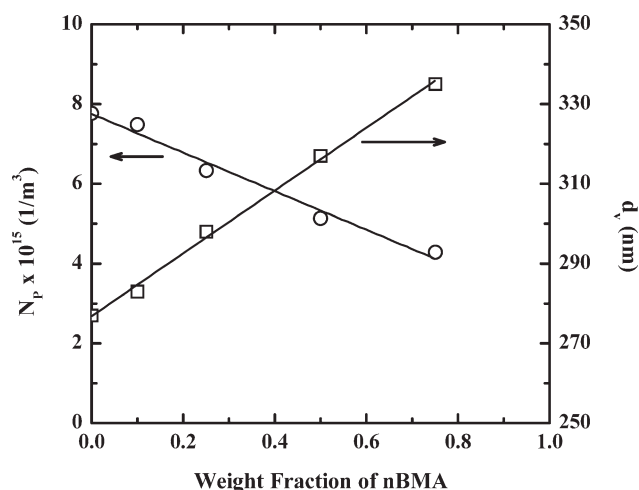


**Figure 5** (○)  $N_p$  and (□)  $\bar{d}_v$  as functions of the weight fraction of nBMA. Experimental data are compared with (—) those predicted with the linear equation.

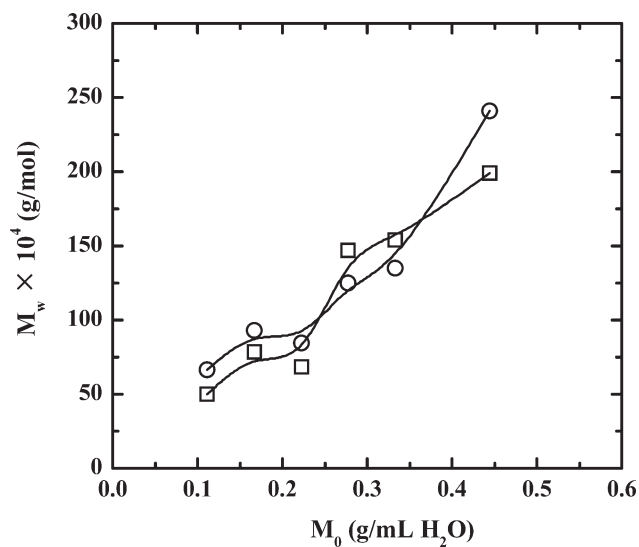


**Figure 6**  $M_w$  values of copolymer submicrospheres with various values of  $M_0$ : (○) P0 series and (□) P0.5 series.

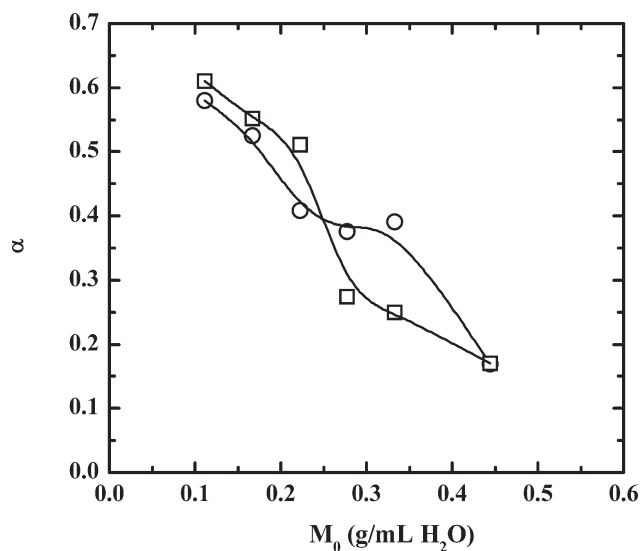


**Figure 7**  $\alpha$  values of copolymer submicrospheres with various values of  $M_0$ : (○) P0 series and (□) P0.5 series.

linearly from 277 to 335 nm, whereas  $N_p$  decreased linearly from  $7.76 \times 10^{15}$  to  $4.29 \times 10^{15} \text{ m}^{-3}$ . Because nBMA dissolved to a lesser extent in the aqueous phase than MMA, the hydrophobicity of the reaction mixture containing nBMA and MMA increased with the weight fraction of nBMA. Therefore, in the initial

stages of polymerization, there existed numerous nucleation sites, so the particle diameter tended to decrease. Thus, in soap-free emulsion polymerization, the particle diameter of the resulting polymers could be controlled by adjustments of the solubility of the monomer in the aqueous phase.<sup>23</sup>

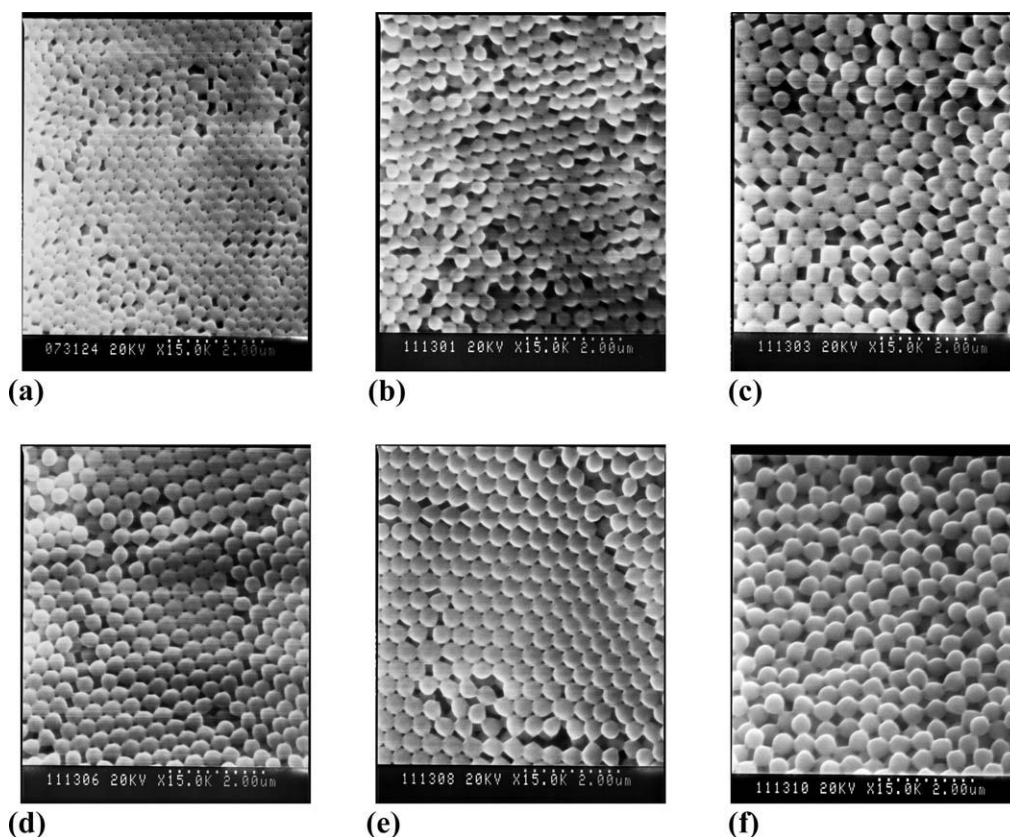


**Figure 8** FESEM images of copolymer submicrospheres with various values of  $M_0$  for the P0 series: (a) 0.11, (b) 0.17, (c) 0.22, (d) 0.28, (e) 0.33, and (f) 0.44 g/mL of  $H_2O$ .

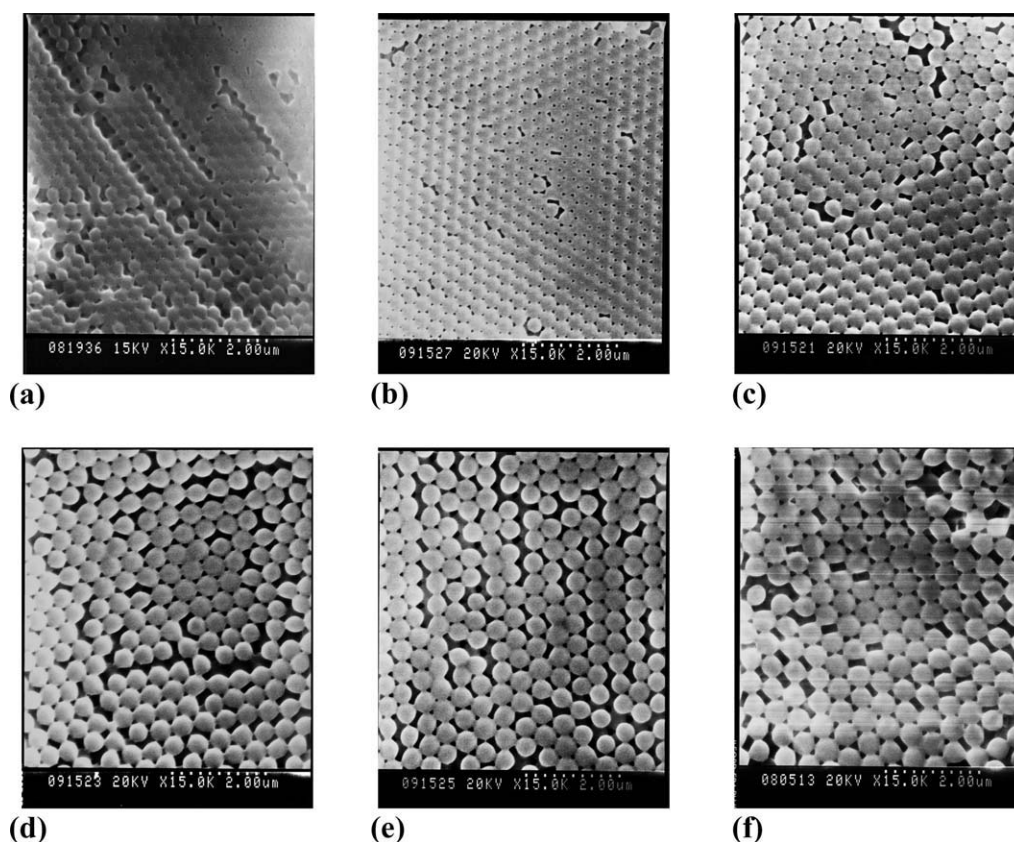


**Figure 9** FESEM images of copolymer submicrospheres with various values of  $M_0$  for the P0.5 series: (a) 0.11, (b) 0.17, (c) 0.22, (d) 0.28, (e) 0.33, and (f) 0.44 g/mL of  $H_2O$ .

### Effect of $M_0$

In this section, we discuss the properties of copolymer submicrospheres prepared with various  $M_0$  values. Figure 6 shows the  $M_w$  values obtained for copolymer submicrospheres with various  $M_0$  values. The  $M_w$  values of the microspheres increased with  $M_0$ , and this suggested that the gel effect became more pronounced with an increase in  $M_0$ .<sup>31</sup> Therefore, the viscosity of the reaction mixture increased during polymerization because of the difficulty involved in the termination step, which was diffusion-controlled.<sup>32</sup> The relationship between the viscosity of the reaction mixture and the molecular weight is given by the Mark–Houwink equation:<sup>28,33</sup>

$$[\eta] = KM^\alpha \quad (7)$$

where  $[\eta]$  is the intrinsic viscosity,  $M$  is the relative molecular weight, and  $K$  and  $\alpha$  are Mark–Houwink constants that depend on the temperature as well as the nature of the polymer and the solvent.

The degree of branching can be determined by a comparison of logarithmic plots of  $[\eta]$  versus  $M$  (Mark–Houwink plots) for polymers with identical chemical structures. Furthermore, these plots indicate that the value of the slope ( $\alpha$ ) for highly

branched polymers is considerably less than that for linear polymers. Normally,  $\alpha$  ranges from 0.65 to 0.75 for a linear random-coil polymer in a good solvent and approaches 0.5 under  $\theta$  conditions. If  $\alpha$  is less than 0.5, the polymer is considered to have a branched structure.<sup>33</sup> The highly branched structure of a polymer sphere possesses many unique properties, such as a huge number of modifiable surface functionalities, lower viscosities, and better solubility, and these spheres have been found to be potentially useful for drug carriers, volume holographic storage, and so forth.<sup>34,35</sup> Figure 7 shows the  $\alpha$  values calculated by GPC–VIS for copolymer submicrospheres obtained with various  $M_0$  values. In the P0 and P0.5 series, the  $\alpha$  values decreased with an increase in  $M_0$ . Because the molecular density increased at high monomer concentrations, branching of the polymer backbone occurred easily during the polymerization reaction.

Figures 8 and 9 show the morphologies of the copolymer submicrospheres in the P0 and P0.5 series with various  $M_0$  values, respectively. The images reveal that the particles were uniform and that the particle diameter increased to several hundred nanometers. Figure 10 shows the relationship between  $\overline{d_v}$  and  $M_0$  for the copolymer submicrospheres in the P0 and P0.5 series. With an

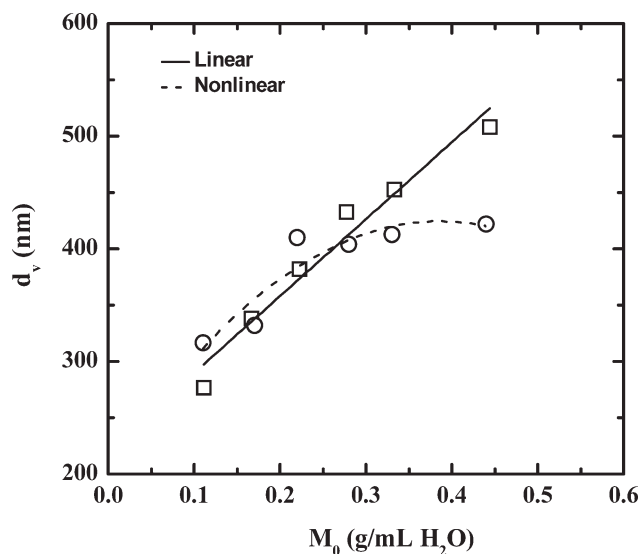


**Figure 10** Particle diameters of copolymer submicrospheres with various values of  $M_0$ : (○) P0 series and (□) P0.5 series. Experimental data are compared with (—) those predicted with the linear equation.

increase in  $M_0$ ,  $\bar{d}_v$  for the P0 series increased from 317 to 422 nm, whereas that for the P0.5 series increased from 277 to 508 nm.  $\bar{d}_v$  in the P0.5 series showed a significant linear increase, whereas that in the P0 series increased and approached the corresponding equilibrium values. The collision frequency of the particles was thought to increase with a high  $M_0$  value during polymerization, and large particles formed because of coagulation. Furthermore, the molecular chains of the polymers in the P0.5 series became flexible ( $T_g = 58.4^\circ\text{C}$ ) during polymerization. Consequently, in the case of the P0.5 series, coagulation occurred easily with an increase in  $M_0$ , and  $\bar{d}_v$  linearly increased. However, the molecular chains of the polymers in the P0 series were not sufficiently flexible ( $T_g = 116^\circ\text{C}$ ); hence,  $\bar{d}_v$  approached the corresponding equilibrium values. In addition, all the  $C_v$  values obtained for copolymer submicrospheres with different  $M_0$  values were less than 4.0%. These results indicate that the copolymer submicrospheres in the P0 and P0.5 series were monodisperse, even when  $M_0$  was increased to 0.44 g/mL of H<sub>2</sub>O during soap-free emulsion polymerization. Thus, the results of this study may provide useful information for the synthesis of monodisperse copolymer submicrospheres with branched structures and different  $T_g$  values by soap-free emulsion polymerization.

### CONCLUSIONS

Monodisperse copolymer submicrospheres with different  $T_g$  values were successfully prepared by soap-free emulsion polymerization. The weight frac-

tions of nBMA played an important role in controlling the various  $T_g$  values of the copolymer submicrospheres.  $T_g$  decreased from 116 to  $26.3^\circ\text{C}$  with an increase in the weight fraction of nBMA and followed the Fox equation. When the weight fraction of nBMA was increased from 0 to 0.75, the particle diameter increased linearly from 277 to 335 nm. On the other hand, when  $M_0$  was increased to 0.28 g/mL of H<sub>2</sub>O, the particle diameters in the P0.5 series showed a significant linear increase, whereas those in the P0 series increased and approached the corresponding equilibrium values. Furthermore, the  $\alpha$  values decreased with an increase in  $M_0$ . Because the molecular density increased at high monomer concentrations, the branched structure of the copolymer spheres occurred easily during the polymerization.

### References

- Cong, H.; Cao, W. *Langmuir* 2003, 19, 8177.
- Wang, D.; Möhwald, H. *Adv Mater* 2004, 16, 244.
- Kitaev, V.; Ozin, G. A. *Adv Mater* 2003, 15, 75.
- Li, H.; Wang, J.; Yang, L.; Song, Y. *Adv Funct Mater* 2008, 18, 3258.
- Kammona, O.; Kotti, K.; Kiparissides, C.; Celis, Y. P.; Fransaer, J. *Electrochim Acta* 2009, 54, 2450.
- Yang, C. H.; Lin, Y. S.; Huang, K. S.; Huang, Y. C.; Wang, E. C.; Jhong, J. Y.; Kuo, C. Y. *Lab Chip* 2009, 9, 140.
- Guo, S. R.; Gong, J. Y.; Jiang, P.; Wu, M.; Lu, Y.; Yu, S. H. *Adv Funct Mater* 2008, 18, 872.
- Tian, E.; Wang, J.; Zheng, Y.; Song, Y.; Jiang, L.; Zhu, D. *J Mater Chem* 2008, 18, 1116.
- Ozin, G. A.; Yang, S. M. *Adv Funct Mater* 2001, 11, 95.
- López, C. *Adv Mater* 2003, 15, 1679.
- Jiang, P.; Mcfarland, M. J. *J Am Chem Soc* 2004, 126, 13778.
- Wong, S.; Kitaev, V.; Ozin, G. A. *J Am Chem Soc* 2003, 125, 15589.
- Mihi, A.; Ocaña, M.; Míguez, H. *Adv Mater* 2006, 18, 2244.
- Foulger, S. H.; Jiang, P.; Lattam, A. D.; Smith, W.; Ballato, J. J.; Dausch, D. E.; Grego, S.; Stoner, B. R. *Adv Mater* 2003, 15, 685.
- Cui, L.; Zhang, Y.; Wang, J.; Ren, Y.; Song, Y.; Jiang, L. *Macromol Rapid Commun* 2009, 30, 589.
- Muranaka, M.; Ono, T. *Macromol Rapid Commun* 2009, 30, 152.
- Yu, Z.; Han, G.; Sun, S.; Jiang, X.; Chen, R.; Wang, F.; Wu, R.; Ye, M.; Zou, H. *Anal Chim Acta* 2009, 636, 34.
- Yang, C.; Guan, Y.; Xing, J.; Shan, G.; Liu, H. *J Polym Sci Part A: Polym Chem* 2008, 46, 203.
- Gu, S.; Akama, H.; Nagao, D.; Kobayashi, Y.; Konno, M. *Langmuir* 2004, 20, 7948.
- Nagao, D.; Sakamoto, T.; Konno, H.; Gu, S.; Konno, M. *Langmuir* 2006, 22, 10958.
- Chen, X.; Cui, Z.; Chen, Z.; Zhang, K.; Lu, G.; Zhang, G.; Yang, B. *Polymer* 2002, 43, 4147.
- Jin, L.; Liu, H.; Yang, W.; Wang, C.; Yu, K. *J Polym Sci Part A: Polym Chem* 2008, 46, 2948.
- Ou, J. L.; Yang, J. K.; Chen, H. *Eur Polym J* 2001, 37, 789.
- Zhang, S.; Zhao, X. W.; Xu, H.; Zhu, R.; Gu, Z. Z. *J Colloid Interface Sci* 2007, 316, 168.
- Gu, Z. Z.; Chen, H.; Zhang, S.; Sun, L.; Xie, Z.; Ge, Y. *Colloids Surf A* 2007, 302, 312.



26. Fox, T. G. *Bull Am Phys Soc* 1956, 1, 123.
27. Fang, S. J.; Fujimoto, K.; Kondo, S.; Shiraki, K.; Kawaguchi, H. *Colloid Polym Sci* 2000, 278, 864.
28. Babac, C.; Güven, G.; David, G.; Simionescu, B. C.; Piskin, E. *Eur Polym J* 2004, 40, 1947.
29. Grunlan, J. C.; Ma, Y.; Grunlan, M. A.; Gerberich, W. W.; Francis, L. F. *Polymer* 2001, 42, 6913.
30. Hong, C. K.; Hwang, M. J.; Ryu, D. W.; Moon, H. *Colloids Surf A* 2008, 331, 250.
31. Ye, Q.; Ge, X.; Zhang, Z. *Radiat Phys Chem* 2003, 66, 11.
32. Zhang, M. G.; Weng, Z. X.; Huang, Z. M.; Pan, Z. R. *Eur Polym J* 1998, 34, 1243.
33. Turner, S. R.; Voit, B. I.; Mourey, T. H. *Macromolecules* 1993, 26, 4617.
34. Suttiruengwong, S.; Rolker, J.; Smirnova, I.; Arlt, W.; Seiler, M.; Lüderitz, L.; Pérez de Diego, Y.; Jansens, P. *J Pharm Dev Technol* 2006, 11, 55.
35. Tomita, Y.; Furushima, K.; Ochi, K.; Ishizu, K.; Tanaka, A.; Ozawa, M.; Hidaka, M.; Chikama, K. *Appl Phys Lett* 2006, 88, 071103.